NJC

Accepted Manuscript

This is an *Accepted Manuscript*, which has been through the Royal Society of Chemistry peer review process and has been accepted for publication.

Accepted Manuscripts are published online shortly after acceptance, before technical editing, formatting and proof reading. Using this free service, authors can make their results available to the community, in citable form, before we publish the edited article. We will replace this *Accepted Manuscript* with the edited and formatted *Advance Article* as soon as it is available.

You can find more information about *Accepted Manuscripts* in the Information for Authors.

Please note that technical editing may introduce minor changes to the text and/or graphics, which may alter content. The journal's standard Terms & Conditions and the Ethical guidelines still apply. In no event shall the Royal Society of Chemistry be held responsible for any errors or omissions in this *Accepted Manuscript* or any consequences arising from the use of any information it contains.

ROYAL SOCIETY OF CHEMISTRY

www.rsc.org/njc

Facile deposition and plasmonic resonance of Ag-Au nanoparticles in titania thin film

Mohan Chandra Mathpal[*1], *Promod Kumar*[2], *Anand Kumar Tripathi*[1], *Balasubramaniyan. R*[3], *Manish Kumar Singh*[4], *Jin Suk Chung*[*3], *Arvind Agarwal*[1]

[1]*Department of Physics, Motilal Nehru National Institute of Technology, Allahabad-211004, India*

[2]*Department of Physics, National Institute of Technology, Hazratbal, Srinagar-190006, India*

[3]*School of Chemical Engineering, University of Ulsan, 93 Daehakro, Namgu, Ulsan 680-749, Republic of Korea*

[4]*Department of Physics, The LNM Institute of Information Technology, Jaipur-302031, India*

*Corresponding authors

Jin Suk Chung; Email: jschung@mail.ulsan.ac.kr, Tel: +82-52-259-2249, Fax: +82-52-259-1689.

Mohan Chandra Mathpal; Email: mohanatnpl@gmail.com, Tel.: +91-532-2271263; Fax: +91-532-2545342.

Abstract

Plasmon resonance in noble metals at nanoscale is technologically important for various applications as it is an important fundamental building block of plasmonic devices. Silver embedded in a glass matrix followed by the deposition of gold embedded in a titania matrix were synthesized in three to four steps by a simple and inexpensive thermal spray pyrolysis technique. The effects of annealing temperature on the plasmonic response and optical activity of silver and gold nanocluster in soda-lime glass and titanium dioxide matrices have been investigated using UV-visible absorption spectroscopy and photoluminescence spectroscopy. The surface plasmon resonance (SPR) at a hybrid metal-dielectric interface for silver and gold was shown to be influenced by the presence of Ag^+ ion and increased particle size of gold nanoparticles as a function of post annealing temperature. This study reveals that the SPR and the luminescence properties are strongly dependent on the glass matrix, which cannot be achieved in all types of glass slides. Field emission scanning electron micrographs confirming the presence of randomly shaped nanoparticles whose size increases with annealing temperature were inconsistent with the particle size calculated from Mie theory.

Keywords: surface plasmon resonance; nanostructures; Spray pyrolysis; optical properties; silver; gold

1. Introduction

The plasmonic nanostructures in the vicinity of multiple semiconducting nanostructures are of great interest due to the squeezing of light beyond the diffraction limit (about half of the wavelength). The unique functionalities such as optical magnetism and a negative index of refraction of plasmonic metamaterials based nanostructures have various applications in nanoantennas, integrated nanophotonics, optical cloaks, sub-diffraction imaging, sub-wavelength waveguides, plasmonic conducting substrates, infrared sensor and nanolasers.[1-5]

These metamaterials are made by the combination or stacking of natural materials such as metals, semiconductors, and dielectrics which are structured in such a way that the sizes of their particular pattern and geometries is much smaller than the operating wavelength in order to yield an artificial material with resonance in absorption to electromagnetic excitation. The plasmonic metamaterials based on noble metals such as silver (Ag) and gold (Au) nanoparticles have unusual dispersion and optical properties. These properties arise from localized surface plasmon resonance (LSPR) in nanostructures. LSPR access a very large range of wave vectors over a narrow frequency band. The origin of this absorption is due to the collective oscillation of conduction band electrons in response to the electrical field of the electromagnetic excitation of light.[3-7] These plasmons are longitudinal surface charge density modes that exist at conducting interfaces in response to optical excitation to support light waves that run along metallic surfaces in surface plasmon resonance (SPR) modes. This SPR wavelength critically depends on the size, shape, inter-particle distance, volume fraction of the metal, and the dielectric constant of the surrounding environment.[6-9] Plasmonic materials based on silicate glasses containing noble metal nanoclusters are exceptionally promising candidates for ultrafast optical switches and modulators. These structures can be fabricated in different matrices including glass for plasmonic resonance of metal nanoparticles by using methods such as ion implantations, thermal ion exchange, melt quenching, sol–gel processing, and other techniques.[9-12] It is well known that the presence of plasmonic nanoparticles (NPs) modifies the antireflection properties of TiO_2 layers.[7] Titanium dioxide (TiO_2) is a high resistive semiconducting oxide material with a wide band gap (anatase: 3.2 eV; rutile: 3.0 eV) has been studied as a promising visible light photocatalyst and photovoltaics material. Due to the large electron–hole recombination on titania (TiO_2) particles, its use as a photovoltaic material is practically difficult.[9-15] There is a lack of literature on the size and matrix dependent plasmonic properties that could be useful in light

trapping photovoltaics for inorganic semiconducting materials by simple and low cost fabrication techniques. Therefore a coherent study has been done here to investigate the plasmonic properties of Ag-Au nanoparticles based semiconducting titania (TiO_2) thin film. In this work firstly, the glass substrate was used as a matrix for the deposition of silver nanoparticles, followed by the deposition of titanium dioxide (TiO_2) thin film, which was further used as a base matrix for the deposition of gold nanoparticles by simple thermal pyrolysis method. This fabrication of a plasmonic metamaterials structure is a new approach for increasing the absorption and trapping of light in semiconducting oxide based thin film, where the film structure exhibits the properties that are usually not found in natural materials, such as negative refractive index of materials.

2. Experimental

The preparation of plasmonic metamaterial based thin film was carried out using a simple and low cost fabrication technique. The microscopic commercial soda lime glass slides (purchased from Marienfeld and Duran Group, both made in Germany) with composition (in approximate weight % of 72.0% SiO_2, 14.0% Na_2O, 0.6% K_2O, 7.1% CaO, 4.0% MgO, 1.9% Al_2O_3, 0.1% Fe_2O_3, 0.3% SO_3) of 0.5 mm thickness were used after cleaning. The silver nanoparticles were first embedded into a preheated microscopic glass substrate at 400°C through deposition by spray pyrolysis technique as reported previously and a detailed process of deposition is also given in the supporting information (SI).[9] Subsequently the TiO_2 layer was deposited by using titanium chloride 1.0 M solution in toluene (2 ml) as a precursor after dissolving in a beaker containing a mixture of distilled water (20 ml) and toluene (20 ml) in a fume hood. This solution was then sprayed 5 times on a preheated plane glass substrate and silver deposited glass substrate at 400°C with N_2 as a carrier gas. After deposition, the titania films were continuously heated on a hot plate for thirty minutes, resulting in a change in the color (reddish-purple) of the glass slide. The TiO_2

thin film prepared on a plane glass substrate (after deposition at 400°C) by spray pyrolysis are termed "TiO_2 film" throughout the paper. The gold nanoparticles were then deposited on these TiO_2 thin films by spraying 5 times at 400°C. The solution for the deposition of gold nanoparticles was prepared by dissolving gold chloride (0.09 gram) (purchased from Sigma Aldrich of 99.9% purity) in a mixture of water (20 ml) and ethanol (20 ml). After the deposition of the gold nanoparticles, the films were maintained at a constant temperature for 4h on the same hot plate at 400°C and the films were then allowed to cool naturally up to room temperature, resulting into the mixture of light red-pink-gold color thin films. The gold coated Ag embedded TiO_2 thin films prepared at this stage (after deposition at 400°C and constant heating for 4h) by spray pyrolysis are termed the "Ag-Au-TiO_2 film" samples. To promote the formation and diffusion of Ag nanoclusters in the glass matrix (or glass substrate) and Au nanoclusters in TiO_2 film (or titania matrix), thermal annealing of the samples was carried out in an electrical tubular furnace at 600°C for two hours in the presence of N_2 gas atmosphere. The "TiO_2 film" annealed at 600°C for 2h in inert atmosphere is termed "TiO_2 annealed film", and the gold coated Ag embedded TiO_2 annealed samples at 600°C for 2h in inert atmosphere is termed "Ag-Au-TiO_2 annealed film". The change in the color of the films after annealing was again observed, and this time the color of the thin films became a light yellowish-pink-gold mixture. For comparison, the role of the matrix in the growth mechanism, the gold nanoparticles were separately deposited on glass substrate and Ag embedded (diffused) glass substrates but the gold nanoparticles did not adhere to the surface and showed a similar morphology as that observed after deposition on titania thin films. All of the experiments were repeated for spray deposition in the presence of N_2 gas atmosphere in a specially designed quartz chamber to avoid from the contamination due to deposition in atmospheric conditions. Schematic illustrations for film deposition in the

presence of N_2 gas atmosphere are shown in Fig. 1(a), and the inset in Fig. 1(b) exhibits the systematic deposition process of plasmonic metamaterials based thin film.

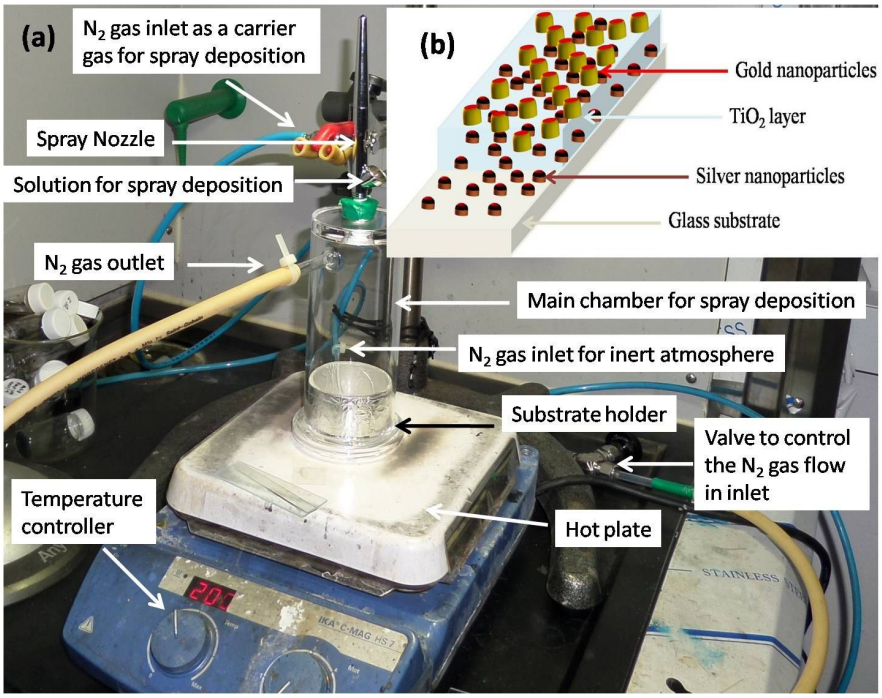

Fig. 1 Illustration of thin film grown using spray pyrolysis method, **(a)** in the presence of nitrogen gas atmosphere and **(b)** the inset represents schematic deposition of Ag-Au-TiO_2 film.

The experiments were repeated in different glass slides and on biological glass from different companies, especially those made in India and South Korea, for spray deposition in atmospheric conditions. However, in most of these, either plasmonic resonance was not exhibited or the silver nanoparticles did not get embedded in the glass matrices. However, the glass slides purchased from the Marienfeld and Duran Group (made in Germany) exhibited similar plasmonic resonance after thermal spraying in atmospheric conditions. The gold-silver nanoparticles formation in TiO_2 thin film deposited on glass matrix (deposited on Marienfeld glass) was studied using X-ray Diffraction (XRD), Raman Spectroscopy, Fourier Transform Infrared Spectroscopy (FTIR), UV-visible Spectroscopy and Photoluminescence

(PL) Spectroscopy, X-ray Photoelectron Spectroscopy (XPS), Field Emission Scanning Electron Microscope (FESEM), and Energy Dispersive X-ray Spectroscopy (EDS) to understand the growth mechanism and the electronic, optical, and plasmonic properties during deposition and thermal annealing in N_2 atmosphere. The typical step-wise details of the synthesis procedure are given in section SI-1 of the supplementary information (SI).

3. Results and Discussion

The XRD plot is shown in Fig. 2 for "Ag-Au-TiO_2 film" and "Ag-Au-TiO_2 annealed film". In both samples, most peak positions are consistent with the diffraction pattern of anatase-TiO_2 (JCPDS file no. 78-2486), and with the pure face centered cubic (fcc) silver structure (with the plane families {111}, {200}, {220}, and {311}, space group fm3m and JCPDS file no. 4-0787). In a previous study, after calcination of the powder sample at 600°C in air atmosphere synthesized by sol-gel method, the anatase-rutile mix phase of TiO_2 (rutile-TiO_2 JCPDS No 21-1276) was observed.[16]

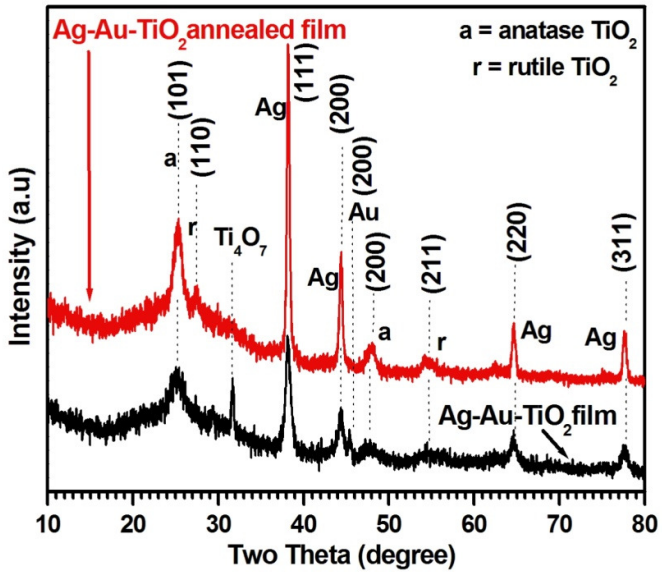

Fig. 2 XRD pattern Ag-Au-TiO_2 film and Ag-Au-TiO_2 annealed film.

An additional impure Ti_4O_7 phase was observed in "Ag-Au-TiO_2 film", which was removed after annealing the sample at 600°C in an inert atmosphere. The presence of an Au-(200) plane (ICDD card no 04-0787) in the form of metal is clearly observed in "Ag-Au-TiO_2 film", but is absent in "Ag-Au-TiO_2 annealed film". This implies that after annealing, the deposited Au nanoparticles entered into the vacant sites of either anatase TiO_2 or rutile TiO_2. The appearance of rutile TiO_2 after annealing may in this case be due to the presence of oxygen vacancies at higher annealing temperature.[16] Other peaks relating to any crystalline impurity (e.g., silver oxide and gold oxide) are absent in the XRD pattern.

Fig. 3 shows the Raman and FTIR spectra for glass substrate: TiO_2 film, TiO_2 annealed film, Ag-Au-TiO_2 film, and Ag-Au-TiO_2 annealed film. The peak positions corresponding to various Raman bands of anatase TiO_2 in TiO_2 film (TiO_2 annealed film, Ag-Au-TiO_2 film, and Ag-Au-TiO_2 annealed film) were assigned to Eg, B1g, and A1g + B1g for six allowed modes.[2,9] In the case of the Ag-Au-TiO_2 film and Ag-Au-TiO_2 annealed film, the anatase TiO_2 peak position shifts and the new additional bands can be seen clearly. These additional peak positions for the samples are mentioned in Table S1 of the supplementary information. The absence and shifting of the few Raman bands in Ag-Au-TiO_2 film and Ag-Au-TiO_2 annealed film was also observed which may be due to the multiphase nanostructures of metamaterials, the different particle size distribution, the shape distribution, morphological variations, discrepancy from stoichiometry, and types of defects that contribute to the changes in the peak position, line width and shape of the mode in the Raman spectrum.[2,3,9] The FTIR spectra show the hydroxyl groups in all the samples is very small, implying that a large fraction of the O–H groups was removed during thermal spray reactions, while small content of vibrational bands such as C–H and C–O bonds is observed in the Ag-Au-TiO_2 film which reduces after annealing of the samples in inert atmosphere.[11-13] The presence of Si–O–Si and Si-O weak band regions corresponding to the bending or stretching mode of the glass

substrate is observed only in a few samples, indicating that most of the thin films are not transparent and they are strongly bonded with the glass substrate. The band around 1210 cm^{-1} due to Ti–O–Ti and Ti–O–Au vibrations has also been observed previously.[14-25] The main FTIR peak positions are mentioned in Table S2 of the supplementary information.

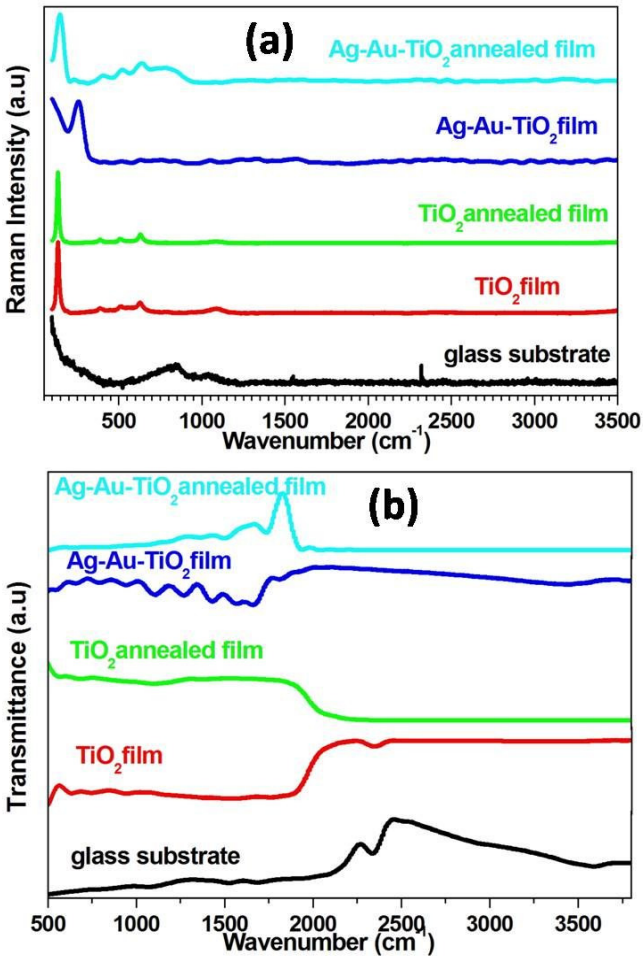

Fig. 3 (a) Raman spectra and **(b)** FTIR spectra of the glass substrate: TiO_2 film, TiO_2 annealed film, Ag-Au-TiO_2 film, and Ag-Au-TiO_2 annealed film.

The absorption spectra for the samples are plotted in Fig. 4(a). The anatase "TiO_2 film" and "TiO_2 annealed film" have an indirect band gap of 3.1 eV (as calculated from the Tauc plots of the indirect energy band gap) because of the transition from the O 2p level in the valence band (VB) to the Ti 3d energy states of the conduction band (CB).[16-17] The formation

of silver and gold nanoparticles is confirmed by the observation of their localized surface plasmon resonance absorption with a maximum at λ = 410 nm and 560 nm, respectively, in the "Ag-Au-TiO_2 film". The intensity of the localized surface plasmon resonance (LSPR) for silver nanoparticles increases after annealing and shows a noisy spectrum of which the maxima is centered at 410 nm. The intensity of the Au LSPR peak at the TiO_2 (semiconductor)-gold (metal) interface after annealing reduces drastically and exhibits a red shift (595 from 560 nm). This is attributed to the increase in the particle sizes of gold nanoparticles as well as to the inter-diffusion of gold nanoparticles inside the titania matrix. Therefore, the annealing after embedding silver into glass and embedding gold into the TiO_2 matrices resulted in the net increase in the refractive index of the surrounding medium. According to Mie theory, the optical absorption α of metal nanoparticles embedded in a medium of refractive index n is given by equation (1).[7]

$$\alpha = \frac{18\pi Q\varepsilon_2 n^3}{\lambda.((\varepsilon_1 + 2n^2)^2 + {\varepsilon_2}^2)} \quad \text{.. (1)}$$

The volume fraction of the nanoparticles is represented by Q, and ε_1 and ε_2 are the cluster-size dependent dielectric constants which are functions of radius (r) and wavelength (λ). The change in the effective refractive index of the film is associated with concentration, pore formation, change in full width at half maxima (FWHM) with the change in particle/cluster size, torques and optical forces on arbitrarily shaped nanoparticles, coupling with the dielectric matrix, nature of matrices, and the defects induced after the removal of the functional group present on the surface of the sample. For a small cluster ($R \leq 10$ nm), the decrease in FWHM with increase in clusters size is due to the mean free path effect of electrons. It has been shown previously that spherical nanoparticles exhibit a dipolar plasmonic resonance at wavelengths where $\varepsilon_m = -2\varepsilon_d$, where ε_m and ε_d are the permittivities of the metal and dielectric, respectively.[9-10,18-21] The resonance condition is satisfied only for

the noble metals such as Ag, Au and Cu nanoparticles at visible wavelengths. Assuming Drude- like the free particles behavior of electrons at nano- sized Ag particles, one can write,

$$R = \upsilon_F \tau$$

Where R is the average radius of the silver nanoclusters and τ is the mean free time (time between two successive collisions) of the conduction electrons at nano-sized metal particles. Spatial confinement and frequent scattering of conduction electrons over the silver nanoparticles dispersed in a transparent glass matrix leads to quantum fluctuations (ΔE) of the average energy of the free electrons around the surface plasmon resonance. Therefore by applying the Heisenberg's uncertainty principle relation ($\Delta E.\ \Delta\tau = \hbar$), the average cluster diameter is calculated from the full width half maximum of the absorption bands using the formula[8]:

$$d = 2\frac{\hbar \upsilon_F}{\Delta E} \qquad (2)$$

where $\hbar$ is the reduced Planck's constant and d is the average diameter of the silver nanoparticles, $V_F = 1.39 \times 10^6$ m/s is the Fermi velocity of electrons in bulk gold and silver (for copper $V_F = 1.57 \times 10^6$ m/s). ΔE (in eV units) is the full width at half maximum of the optical absorption band. The average radii size of Ag and Au nanoclusters for "Ag-Au-TiO_2 film" was calculated as 2 nm and 3 nm, respectively, using the formula derived from the Mie theory of plasmonic resonance for spherical nanoparticles, as given in equation (2)[10-13]. The average size of Ag nanoclusters is 8 nm for "Ag-Au-TiO_2 annealed film". Equation (2) is valid provided the size of gold clusters is much smaller than the mean free path of the electrons in the bulk metal. The mean free path of the electrons is about 27 nm at room temperature for bulk silver and 20 nm for bulk gold.[12-13] Therefore, the as deposited films after annealing show a typical interference-like behavior for the deposited films. This confirms the structural analysis since no Au nanoparticles are expected to induce the SPR effect after the annealing due to the increase in the size of the Au nanoparticles.[7,18-22]

Fig. 4(b) shows the PL spectra for the Ag-Au-TiO_2 film and the annealed film in order to understand the SPR activity of Ag and Au nanoparticles. The PL emission peaks were obtained within the visible range with peak positions at 405, 521, and 661 nm and in the IR range with peak position at 854 nm for the Ag-Au-TiO_2 film.

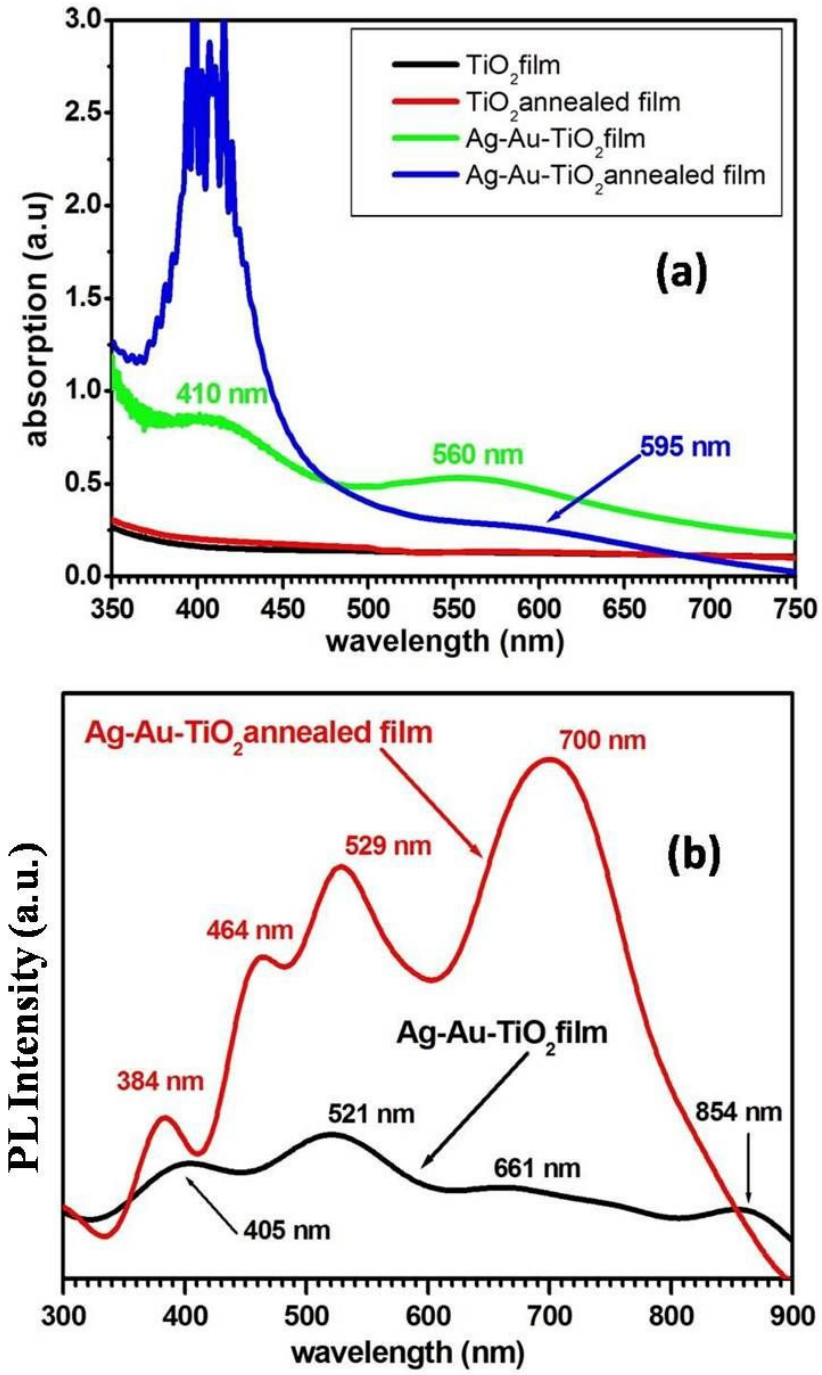

Fig. 4 (a) UV-Vis absorption spectra of the TiO_2 film: TiO_2 annealed film, Ag-Au-TiO_2 film, Ag-Au-TiO_2 annealed film and, **(b)** PL spectra of Ag-Au-TiO_2 film and Ag-Au-TiO_2 annealed film.

In Ag-Au-TiO_2 annealed film all the PL emission peaks were found within the visible range with peak positions at 384, 464, 529, and 700 nm, respectively, which were either blue

shifted or red shifted with respect to the Ag-Au-TiO_2 film. [22-25] The first emissions in both the film at 405 and 384 nm are attributed to the near band edge transition and direct transition from the conduction band to the valence band of TiO_2. To the best of our knowledge from the literature survey, the Ag^0 and Au^0 atoms do not exhibit any luminescence properties. In addition, the PL emissions in the Ag based ion-exchange matrix are known to be luminescent in both crystalline and glassy matrices due to the presence of Ag^+ ions. This suggests that silver becomes embedded into the soda-lime glass substrates during thermal spray by the diffusion of Ag^+ ions in the ion exchange process.[22-34] The ion exchange process also occurs at low temperatures between Ag^+ and Na^+ in the glass matrices, with the subsequent inter-diffusion of the two species in order to maintain the electrical neutrality of the glass. Therefore, to understand the Ag-Au plasmonics behaviors and luminescence mechanism, XPS was carried out for "Ag-Au-TiO_2 film" and "Ag-Au-TiO_2 annealed film".

Fig. 5(a) to 5(f) show the comparative XPS core level spectra of the main compositional elements present in glass matrix for the Ag-Au-TiO_2 film and Ag-Au-TiO_2 annealed film. The other details regarding XPS, comparative general scan spectra for both the film and the peak positions for binding energies of annealed film, are mentioned in section SI-4 of the supplementary information. Based on the general scan and core level spectrum, the presence of C-1s (285.48 eV) and O-1s (~531.7 eV) due to the formation of anatase TiO_2 and Ti_4O_7, and the presence of Si-2p (~102.18 eV) due to the presence of silicates in glass matrix are evident and show clear peak positions for Ag-Au-TiO_2 film, whereas the peaks of Ag, Au, and Ti are not detectable in this film. These absent peaks emerge after annealing the film, whiles the others peaks get shifted after annealing in the N_2 atmosphere. The carbon contamination has been significantly reduced after annealing and the peak position also gets shifted. The core level spectra of the annealed film shows C-1s (at ~284.58 eV), O-1s (~530.2 eV), Ti-$2p_{3/2}$ (~458.98 eV), Ti-$2p_{1/2}$ (~464.68 eV), Ag-$3d_{3/2}$ (~373.68 eV), Ag-$3d_{5/2}$ (~367.68

eV), Si-2p (~102.28 eV), Au-4$f_{7/2}$ (~83.78 eV), and Au-4$f_{5/2}$ (~87.48 eV) positions, indicating the presence of compositional elements.[22-30] The Ti-2$p_{3/2}$ peak position corresponds to TiO bonding in film as is also evident by XRD. The annealed film illustrates spin–orbit splitting of the Ag-3d and Au-4f levels, manifested as Ag 3$d_{3/2}$, Ag 3$d_{5/2}$, and Au-4$f_{5/2}$, Au-4$f_{7/2}$, respectively. The difference between the two Ag peaks is 6.0 eV, while 3.7 eV between the two Au peaks confirms the incorporation of Ag-Au in metallic form in the glass- TiO_2 matrix, respectively. In addition, the chemical shift of ~0.32 eV was observed for the Ag-3d peak position towards low binding energy, while the shifting of ~1.5 eV in O-1s (from 531.7 to 530.2 eV), ~0.48 eV in Ti-2p (from ~458.5 to ~458.98 eV)[26], and ~0.1 eV in Si-2p was also observed. This clearly indicates that the silver is also present in the form of Ag^+ for the formation of silver oxide (Ag_2O), as the required Ag 3d binding energy for this compound is in the range of 367.6 ~367.7 eV.[26-33] In some studies, it was observed that the chemical states of Ag associated with the Ag 3$d_{5/2}$ in Ag-doped TiO_2 samples exist mainly as Ag^0 (metallic Ag) at 367.9 or 368.1eV, Ag^{2+} (AgO phase) at 367.0 or 367.8 eV and Ag^+ (Ag_2O phase) at 367.6 or 367.7 eV in the XPS signals, respectively.[22,24,26] The presence of the Ag_2O phase could not be detected by XRD as it may be present in a very small amount at the interface of the TiO_2 layer and Ag embedded glass substrate. The chemical shift in the Ti 2p and O 1s peak position is attributed to the presence of impurity elements such as chlorine, carbon, and small residual functional groups (when the matrix is annealed at 600°C) from the precursors present in the glassy network. This is evident from Raman and FTIR spectra, general scan XPS spectra, and EDX pattern as shown in sections SI-2 to SI-5 of the supplementary information.[17] The shifting and reduction in intensity of the Si 2p peak position after annealing confirming the change in the chemical environment of silicates (mainly Si-O bonding) in the glass matrix indicates that the Ag ions are successfully embedded in the glass matrix through the ion- exchange process.[24-34]

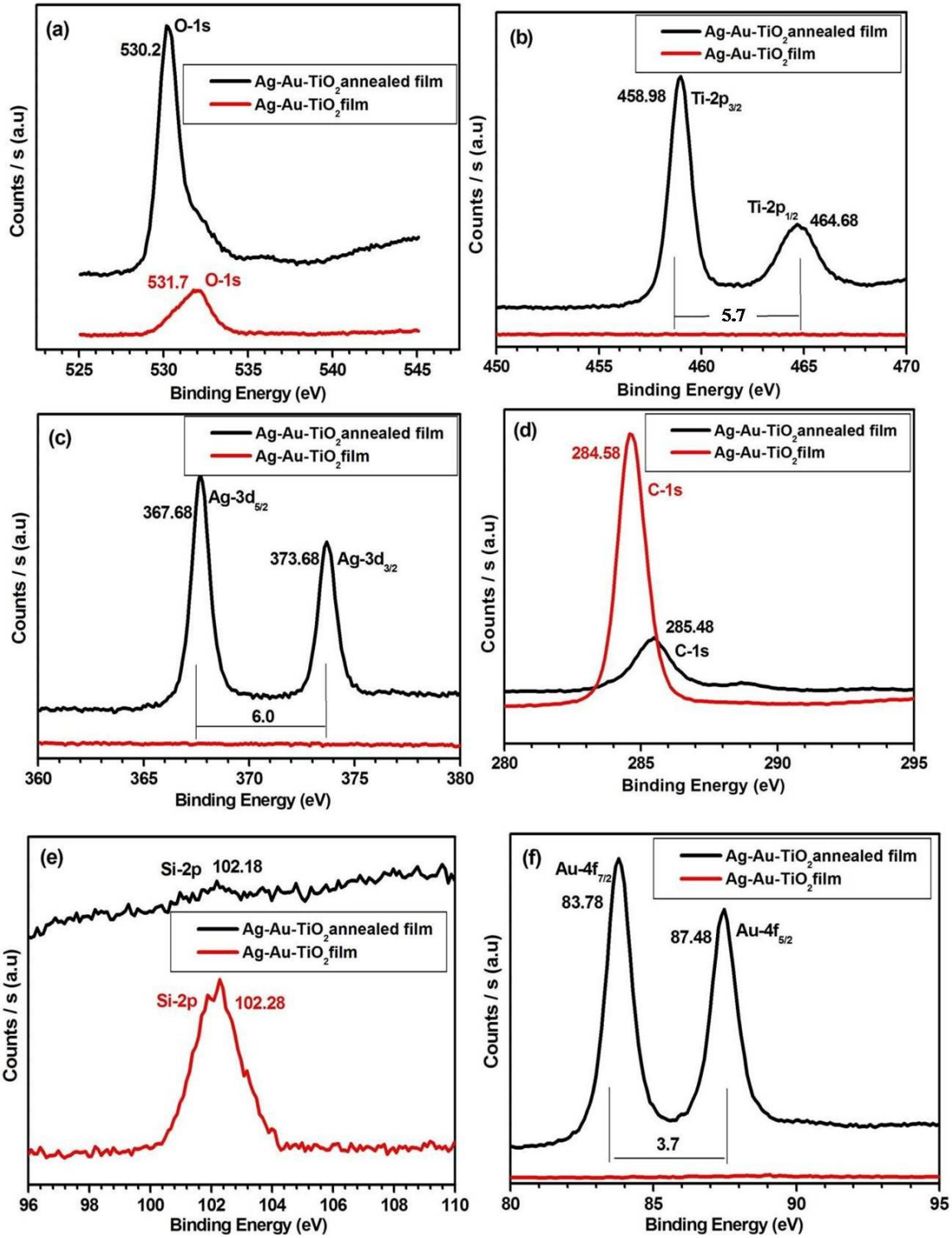

Fig. 5 XPS core level spectra of elements in Ag-Au-TiO_2 film and Ag-Au-TiO_2 annealed film: **(a)** oxygen (O), **(b)** titanium (Ti), **(c)** silver (Ag), **(d)** carbon (C), **(e)** silicon (Si), and **(f)** gold (Au).

As expected, the possible explanation for the plasmonics behaviors and PL emissions is now easy to understand due to the presence of Ag^+ ions in annealed film. This is also well supported by the change in the colors of the thin film (from reddish to light yellowish) after annealing as Ag^+ ions are unstable and can be reduced even at low temperatures.[22] Since the Ag^0 atoms remain in the annealed film, the Ag^+ ions that cause the luminescence must be present in the soda-lime glass or at the interface. The increase in PL intensity observed for the annealed film at 600°C is correlated with the higher concentration of Ag^+ ions after the thermally activated oxidation of silver. The main difference between pure silica glass and silica based other commercially available glass is the compositional variations and presence of network modifiers for diffusion of silver and other metal ions. The presence and role of these network modifiers such as Mg, Ca, and Na for soda-lime glass is very crucial during deposition and annealing process as evident from the general scan XPS and EDX pattern. Thereby the glass slides purchased from the Marienfeld and Duran Group (made in Germany) exhibited the plasmonic properties which are not achievable and all other kind of glass slides. These elements in the form of network modifiers are responsible for the generation of oxygen vacancy, defects, and non-bridging oxygen with unsaturated bonds, which act as pinning centers for the Ag^+ ions to exhibit the PL emissions.[22-24] Therefore, the emission signals due to the presence of Ag^+ ions at 464, 483, 494, 521, 529, 661, and 700 nm originate either from the radiative recombination or from the charge transfer transition from an oxygen vacancy trapped electron and may be a mixture of these two in the "Ag-Au-TiO_2 film" and "Ag-Au-TiO_2 annealed film". These Ag ions in the form of Ag_2O nanoparticles may form a core-shell type structure with Ag^0 as a core at the metal-glass-TiO_2 interface, and thus a hybrid metal-dielectric interface is constructed to generate a noisy plasmonic resonance of silver-silver ion based nanoparticles. A detail study of noisy and anomalous plasmonic resonance and photoluminescence in Ag based hybrid matrices will be reported elsewhere in our future

work. The stability of the plasmonic behavior of these Ag embedded glass matrices followed by the coating of TiO_2 and gold nanoparticles was tested at certain time intervals. The UV-Vis absorption spectra of the films collected after a period of two month show similar absorbance behavior as that of thin films, indicating that gold and silver nanoparticles are stable with glass-TiO_2 within that time frame. All these results suggest that Ag-Au-TiO_2 thin film gives an advanced plasmonic metamaterial based semiconducting thin film which may be useful for superior light trapping low-cost photovoltaics and other optoelectronic applications.

To understand the growth processes and the morphological changes of without annealed and annealed film during the film formation, the thin films were characterized at different stages by field emission scanning electron microscopy (FESEM) at different magnifications as shown in Fig. 6. The micrographs indicate that the TiO_2 thin film has cavities similar to a honeycomb structure, and is bonded to the glass substrate. Upon subsequent deposition of Au nanoparticles on the TiO_2 film, the gold nanoparticles became embedded inside the TiO_2 nanostructures, thus the film works as an active adsorptive centre for the deposition of Au nanoparticles. It is clearly seen that the dispersion of the gold nanoparticles is homogenous and the gold nanoparticles are well attached on the surface of the as-deposited TiO_2 thin film. It is clearly observed that the sizes of Au nanoparticles grown on the TiO_2 matrix increase after annealing (white particles in micrographs). Fig. 6(d) shows that the morphology for Au nanoparticles in annealed thin film is similar to the morphology reported previously.[7] The size of gold NPs in each image was measured individually. The particle shape and size distribution is random and is not perfectly spherical for the nanoparticles of different sizes. The Au particles size before annealing in the TiO_2 matrix was in the range of 12 to 24 nm which increases on an average in the range of 38-75 nm after annealing at 600°C in an inert atmosphere. The results are not consistent with the particle size as calculated from the UV-

absorption on the basis of Mie theory, due to the difference in shape of the nanoparticles, but the results concur that the gold particle size in the range of 38-75 nm cannot give plasmonic resonance. This illustrates the fact that for gold plasmonic absorbance, the particle size should be quite small.[7] The film thickness was measured using the FESEM cross-sectional area image of the thin film. The film thickness for gold coated TiO_2 thin film was observed to

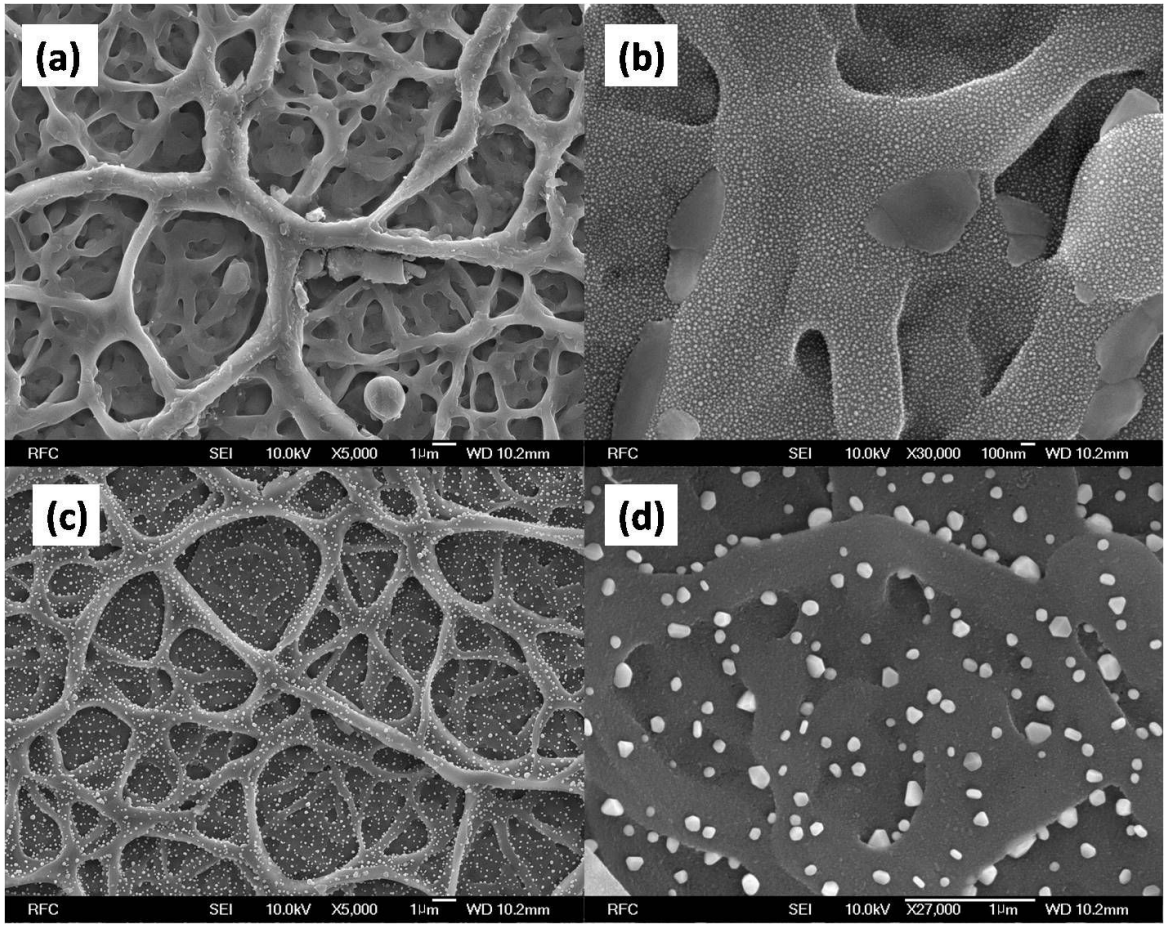

Fig. 6 FESEM of **(a)** Ag-Au-TiO_2 film at 1 μm scale, **(b)** Ag-Au-TiO_2 film at magnified scale of 100 nm, **(c)** Ag-Au-TiO_2 annealed film at 1 μm scale, and **(d)** Ag-Au-TiO_2 annealed film at magnified scale of 1μm.

be 997±13 nm by taking the FESEM micrographs from the cross-sectional area of the "Ag-Au- TiO_2 annealed film", as shown in section SI-5 of the supplementary information. The chlorine impurity was identified in the EDX pattern on the surface of all the samples due to

the precursor used in synthesis, and does not play a major role here for the plasmonic behavior of silver-gold nanoparticles.

On the basis of above results the formation mechanism of the film can be briefly explained here. The photographs for the formation of film at different stage are shown in Figure 7. The silver nanoparticles were deposited first by thermal spray method on glass substrates (Fig. 7(a)). After spray deposition the continuous heating of the slides for an hour helped the silver ions to get incorporated in to the glass materials by ion-exchange process.[3] Silver ions diffuses up to several micrometers in the soda-lime silicate glass during the ion-exchange process. It has been observed that during the process silver ions partly reduce the neutral silver atom species, possibly aggregating to form silver nanoclusters inside the glass matrix and its coloration is shown in Fig. 7(b).[8,35] The following equation presents the possible diffusion mechanism for silver exchange in soda-lime glass;

$$\textbf{Glass + heating} \longrightarrow \mathbf{h^+ + e^-}$$

$$\mathbf{Ag^+ + e^-} \longrightarrow \mathbf{Ag^0}$$

where h^+ is a hole and e^- is the electron.[36] During the deposition, the glass samples were colorless and when the substrates were just removed after deposition then the films had no measurable absorption in the visible region.

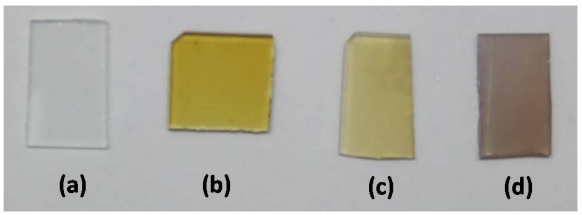

Fig. 7 Photographs of **(a)** glass substrate, **(b)** Ag nanoparticles deposited on glass substrate, **(c)** Ag-TiO_2 film (matrix) and **(d)** Ag-Au-TiO_2 annealed film.

There was a lack of significant surface plasmon resonance (SPR) of silver nanoclusters in the glass during ion-exchange process in these experimental conditions, indicating the silver aggregation did not occur. The soda-lime silicate glass coloring starts after the ion-exchange process takes place in the experiment, and it takes around an hour of heating or longer than this time. Once the coloration has appeared after exchange process then TiO_2 film was deposited and heated for some time. The appearance of this Ag-TiO_2 film (matrix) is shown in Fig. 7(c). Finally the gold nanoparticles were deposited by spray pyrolysis and annealed in a furnace as explained in experimental details and supporting information. During the annealing process Au ions and nanoparticles diffuses into Ag/TiO_2 matrix and results into the Ag-Au- TiO_2 annealed film as shown in Fig. 7(d). There is a faint plasmonic resonance for Au nanoparticles in this film at 595 nm as the resonance at SPR frequency strongly depends on the dielectric function as well as the nanoclusters size and composition.[35-37] Therefore the plasmonic properties observed here are of special interest due to ease of deposition by cost effective techniques on glass substrate.

4. Conclusions

In conclusion, plasmonic metamaterials based Ag-Au-TiO_2 thin film on cost effective soda-lime glass can be produced in a simple, fast, and inexpensive way by using a novel three to four stage thermal spray pyrolysis method. This results in plasmon resonance of silver and gold nanoparticles. The annealing in inert atmosphere affects the plasmonic resonance of both silver and gold nanoparticles. It shows the possibility to control the concentration, shape and average size of the plasmonic nanoparticles by controlling the precursor concentration and deposition conditions such as pressure and temperature etc. Thus, the bonding of Ag-Au-TiO_2 thin film can significantly trap the light of a particular wavelength by means of plasmonic resonance for nonlinear optics, sensing, and superior photovoltaic and optoelectronic applications. It has been observed that Ag^+ ions diffuse in pure silicates

matrices during thermal spraying and annealing processes, most of them reduced to Ag^0 and subsequently forming silver metallic nanoparticles along with the Ag_2O phase, even in inert atmospheres of N_2 gas. The Ag^+ ion gives characteristic PL emissions due to the presence of network modifiers in the form of non-bridging oxygen in the TiO_2 based glassy matrix. It illustrates that the plasmonic resonance and the luminescence properties are strongly dependent on the glass or on the composition of dielectric matrices.

Acknowledgement:

This research was supported by the Basic Science Research Program (NRF 2011-0022485) and Korea-India Exchange Student Program (2013 Global Korea Scholarship) funded by the Ministry of Education of Republic of Korea. Mohan Chandra Mathpal is also thankful to the director at MNNIT for providing the characterization facility and funding support through TEQIP-II project for carrying out the research work.

Supporting Information (SI): Supporting information is available.

Declarations:

The authors declare that there is no competing financial interest.

References

[1] Kreibig, U.; Vollmer, M. Optical Properties of Metal Clusters, Springer, Berlin, **1995**.

[2] Mathpal, M. C.; Tripathi, A. K.; Singh, M. K.; Gairola, S. P.; Pandey, S. *Chem. Phys. Lett.*, **2013**, *555*, 182–186.

[3] Kelly, K. L.; Coronado, E.; Zhao, L. L.; Schatz, G. C., *J. Phys. Chem. B*, **2003**, *107***,** 668–677.

[4] Philipp, R.; Kumar, G. R.; Sandhyarani, N.; and Pradeep, T., *Phys. Rev. B*, **2000**, *62*, 13160-13166.

[5] Jia, H.; Zeng, J.; Song, W.; An, J.; and Zhao, B. *Thin Solid Films*, **2006**, *496*, 281-287.

[6] Ren, F.; Jiang, C.; Liu, C.; Fu, D.; Shi, Y., *Solid State Commun.,* **2005**, *135*, 268-272.

[7] Pedrueza, E.; Valdés, J. L.; Chirvony, V.; Abargues, R.; Saz, J. H.; Herrera, M.; Molina, S. I.; Pastor, J. P. M. *Adv. Funct. Mater.*, **2011**, *21*, 3502–3507.

[8] Mathpal, M. C.; Kumar, P.; Kumar, S.; Tripathi, A. K.; Singh, M. K.; Prakash, J.; Agarwal, A. *RSC Adv.,* **2015**, *5*, 12555 - 12562.

[9] Mathpal, M. C.; Kumar, P.; Balasubramaniyan, R.; Chung, J. S.; Tripathi, A. K.; Singh, M. K.; Ahmad, M. M.; Pandey, S. N.; Agarwal, *Mater. Lett.,* **2014**, *128*, 306- 309.

[10] Manikandan, P.; Manikandan, D.; Manikandan, E.; Ferdinand, A. C., *Plasmonics*, **2014**, *9*, 637-643.

[11] Sheng, J., *Int. J. Hydrogen Energy,* **2007**, *32*, 2602 – 2605.

[12] Karthikenyan, B., **2008**, *103*, 114313.

[13] Alvarez, M. M.; Khoury, J. T.; Schaaff, T. G.; Shafigullin, M. N.; Vezmar, I.; Whetten, R. L. *J. Phys. Chem. B,* **1997**, *101*, 3706-3712.

[14] Wen, Y.; Ding, H.; and Shan, Y.; *Nanoscale*, **2011**, *3*, 4411-4417.

[15] Bineesh, K. V.; Kim, D. K.; and Park, D. W., **2010**, *2*, 1222-1228.

[16] Tripathi, A. K.; Singh, M. K.; Mathpal, M. C.; Mishra, S. K.; Agarwal, *J. Alloy. Compd.*, **2013**, *549***,** 114-120.

[17] Medda, S. K.; De, S.; De, G., *J. Mater. Chem.*, **2005**, *15*, 3278–3284.

[18] Ji, A.; Raziman, T. V.; Butet, J.; Sharma, R. P.; Martin, O. J. F. *Opt. Lett.*, **2014**, *39(16)*, 4699-4702.

[19] Kim, S. J.; Thomann, I.; Park, J.; Kang, J. H.; Vasudev, A. P.; Brongersma, M. L. Light, *Nano Lett.*, **2014**, *14*, 1446−1452.

[20] Schuller, J. A.; Barnard, E. S.; Cai, W.; Jun, Y. C.; White, J. S.; Brongersma, M. L., *Nat Mater.* **2010**, *9*, 193-204.

[21] Chalabi, H.; Schoen, D.; Brongersma, M. L., *Nano Lett.*, **2014**, *14*, 1374−1380.

[22] Garcia, M. A.; Heras, M. G.; Cano, E.; Bastidas, J. M.; Villegas, M. A.; Montero, E.; Llopis, J.; Sada, C.; Marchi, G. D.; Battaglin, G.; Mazzoldi, **2004**, *96(7)*, 3737-3741.

[23] Vasireddy, R.; Paul, R.; Mitra, A. K., **2012**, *2*, 1-6.

[24] Xu, K.; Heo, J.; Chung, W. J., *Int. J. Appl. Glass Sci.,* **2011**, *2(3)*, 157–161.

[25] Rahulan, K. M.; Ganesan, S.; Aruna, P. *Adv. Nat. Sci.: Nanosci. Nanotechnol.*, **2011**, *2*, 025012-025017.

[26] Wagner, C. D.; Riggs, W. M.; Davis, L. E.; Moulder, J. F. handbook of X-ray photoelectron spectroscopy. Published by Perkin-Elmer Corporation, physical electronics division.

[27] Swamy, V.; Muddle, C. B.; Dai, Q. *Appl. Phys. Lett.*, **2006**, *89*, 163118-21.

[28] Ferrari, A. C.; Basko, D. M. Raman., *Nat. Nanotechnol.*, **2013**, *8*, 235- 246.

[29] Zhang, H.; Fan, X.; Quan, X.; Chen, S.; Yu, H., *Environ. Sci. Technol.,* **2011**, *45*, 5731-6.

[30] Neto, A. H. C.; Guinea, F.; Peres, N. M. R.; Novoselov, K. S.; Geim, A. K. *Rev. Mod. Phys.,* **2009**, *81*, 109- 162.

[31] Pivin, J. C.; García, M. A.; Hofmeister, H.; Martucci, A.; Vassileva, M. S.; Nikolaeva, M.; Kaitasov, O.; Llopis, J. *Eur. Phys. J. D*, **2002**, *20*, 251- 260.

[32] Brigss, D.; and Seah, M. P. Practical Surface Analysis, Auger and X-ray Photoelectron Spectroscopy, 2nd ed.(Wiley, Chichester), **1990**, *1*, 595–634.

[33] García, M. A.; Paje, S. E.; Villegas, M. A.; Llopis, J. *Mater. Lett*. **2000**, *43*, 23- 26.

[34] Hofmeister, H.; Thiel, S.; Dubiel, M.; Schurig, E., *Appl. Phys. Lett.* **1997**, *70(13)*, 1694-1696.

[35] Kumar, P.; Mathpal, M. C.; Tripathi, A. K.; Prakash, J.; Agarwal, A.; Ahmad, M. M.; Swart, H. C., *Phys. Chem. Chem. Phys.* **2015**, *17 (14)*, 8596-8603.

[36] Sheng, J.; Zheng, J.; Zhang, J.; Zhou, C.; Jiang, L., *Physica B,* **2007,** *387,* 32.

[37] Standridge, S. D.; Schatz, G. C.; Hupp, J. T., *Langmuir*, **2009**, *25*, 2596.